Journal of Constructional Steel Research 198 (2022) 107534

Contents lists available at ScienceDirect

Journal of Constructional Steel Research

journal homepage: www.elsevier.com/locate/jcsr

Experiment and numerical modelling of a demountable steel connection system for reuse

Xianghe Dai *, Jie Yang, Dennis Lam, Therese Sheehan, Kan Zhou

Faculty of Engineering and Informatics, University of Bradford, Richmond Road, Bradford BD71DP, UK

ARTICLE INFO

Keywords:
Steel reuse
Block shear connector
Demountable
Standardisation
Experimental study
Finite element modelling

ABSTRACT

Currently, steel reuse is only a marginal practice. To facilitate deconstruction and efficient reuse of steel components, an innovative connection system was proposed. This system adopts a 'Block Shear Connector (BSC)' that allows beam length to be standardised and suitable for a wide range of different sizes of the supporting members within the same planning grid. This paper presents the experimental and numerical studies of a beam-to-beam connection using BSCs. The BSC used was made from a standard universal HE / UC section and was bolted to the beams by using partial depth end plates. The experimental results provided the shear resistance, moment-rotation, failure behaviour, demountability and reusability of the steel components. Further numerical simulation conducted investigated the effect of some key parameters (steel strength, thickness of BSC web, thickness of BSC flange, initial bolt stress) on the behaviour of the connections. The results obtained highlighted the demountability of this innovative bolted connection system and the reusability of structural components.

1. Introduction

Steel is a highly recyclable construction material, but it is also energy and carbon intensive in production, as the recycling process consumes a massive amount of energy and generates a large volume of carbon dioxide emissions. Over recent years, sustainable building techniques have been considered and recommended in the construction industry to reduce waste and reuse materials more efficiently without recycling. Demountability of construction systems, especially steel framed building systems, is very important as it allows structural parts to be reused without the need for recycling. Steel structures are inherently adaptable and demountable with the potential to reuse components. Connection between steel frame systems is a key member which allows the adaptability of construction member reuse.

Estimated recycling rate of steel construction products arising from the demolition of buildings in the UK is on average 91%, whilst the proportion by mass of elements reused is low (5%) and declining [1]. Recycling steel saves only approximately 50% of the energy and carbon over making new steel [2]. Reusing steel components, however, generally needs minor reprocessing and less energy consumption for reclamation, and has significant contribution to the efficient use of materials. Simple geometries and standard detailed design for the steel structures obviously have the potential to make reuse easier, profitable and more mainstream. For steel frame construction, attention has been paid to a greater standardisation of the connections since the past two decades as the connections are of the most influential items [3]. Particular interest for standardised design for reuse / deconstruction shown in this paper goes to the framed structures, the most commonly used building construction form in the UK, to maximize the contribution of steel reuse to sustainability and resource efficiency.

Conventional simple connections, such as the most preferably used [4] flexible end-plates and fin plates, provide a significant degree of simplicity and standardisation compared to moment-resisting connections [5] and thus easier to reuse, however, it is unlikely that they are compatible with different structural elements in different buildings when the members are dis-assembled and reused in-situ or relocated after the structure comes to the end of service life.

Traditional connection using end plates and bolts has been extensively investigated [6–17] and well employed in building practices, but reuse of connected members after service life and replacement during service life are rarely considered. The innovative connection presented in this paper adopts a 'Block Shear Connector (BSC)' manufactured from standard HE / UC sections and bolted to the connecting members (using end plates at the beam ends). It keeps the benefits of simple connections such as easy and economic fabrication in the workshop, easy and rapid erection and deconstruction on site. More importantly, it allows beam

* Corresponding author.
E-mail address: x.dai@bradford.ac.uk (X. Dai).

https://doi.org/10.1016/j.jcsr.2022.107534
Received 7 June 2022; Received in revised form 26 August 2022; Accepted 29 August 2022
Available online 7 September 2022

length to be standardised and suitable for a wide range of column sizes within the same planning grid. In addition, it saves beam coping cost when connecting to beams and is replaceable since it is completely demountable. The BSC is adaptable and can be used to connect open steel sections, hollow steel sections or box sections, allowing for variations in the length of the beams and profiles of the columns so that facilitate re-use of the steel components.

This paper presents the experimental and preliminary numerical studies on this innovative connection. Ease of demountability and the reusability of the steel components were highlighted from the test observations. Obtained shear resistance, moment-rotation and failure behaviour were employed to validate developed finite element models. Further parametric study was conducted to investigate the effect of some key parameters (steel strength, thickness of BSC web, thickness of BSC flange, initial bolt stress) on the behaviour of this type of connection.

2. Experimental study

In the research presented in this paper, the Block shear connector (BSC) is specially designed to use for both beam-to-beam connections and beam-to-column (H/I section) connections. Fig. 1 shows a beam-to-beam connection where a stub section is used as the BSC to transfer shear force from the secondary beam to the primary beam. Bolts were used to connect the BSC to the web of the primary beam and the partial-depth end plate which was welded to the secondary beam. The BSC connection provides flexibility in connection geometries and could bridge the beam members to primary beams and a wide range of column profiles. Therefore, the BSC could facilitate standardisation in beam length within a same planning grid, for example, multiple of 1.5 m for UK practice. Using bolted connections, the structure is easy de-construct-able and elements replaceable. The specimen was designed as a nominally pinned connection where the necessary rotation capacity could be provided by the deformation of the BSC and connected plates.

Two experimental tests were conducted under ultimate limit conditions. In the first test, propped construction technique was used. To achieve this, the specimen was assembled on the laboratory floor and all three beams were supported during fabrication. Then the assembly was lifted to the roller supports. This test was terminated after the connectors failed. Then, the specimen was dismantled and the damaged BSC was demounted and replaced by new BSCs. The second specimen was fabricated using unpropped construction technique. To do this, the primary beams were resting on the roller supports while the secondary beam was lifted by using the crane, and the bolts were initially in contact with the bolt holes in the maximum degree (clearances still exist due to manufacturing imperfections, e.g. possible bowling and twisting of the end plates caused by welds shrinkage, etc.). The specimen details, test setup, loading regime, instrumentation and experimental observations and results are described in the following subsections.

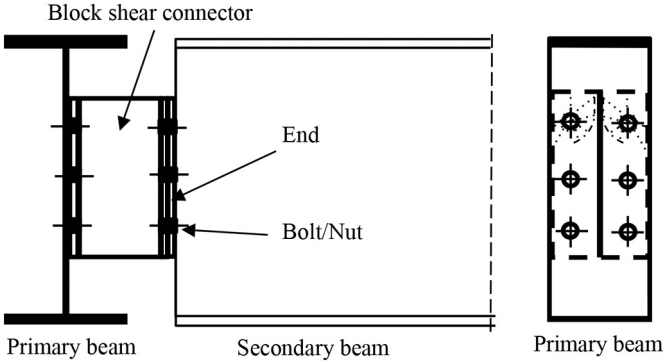

Fig. 1. Sketch of the beam-to-beam BSC connection.

2.1. Specimen details

The specimens were designed to comprise a secondary beam with beam ends connected to the primary beams, and was designed as a nominally pinned joint where the necessary rotation capacity can be provided by the deformation of the BSCs and the connected plates. Fig. 2 illustrates the BSC specimen assembly and components. Components of the specimen included primary beams, secondary beam with partial end plates, BSCs, bolts/nuts and transverse web stiffeners. Table 1 summarises the profile, quantity and material of the components used for one specimen. The BSCs were manufactured from a standard UC section (152×152×23) and were bolted to the web of the primary beams and the partial depth end plates welded to ends the secondary beam with 6 mm fillet welds. The M20 bolts were placed nominally 90 mm apart with the edge distance of 30 mm. The vertical spacing of the bolts was set as 75 mm and the edge distance was 50 mm. The pre-drilled bolt holes were 22 mm in diameter. The torque applied to individual bolt was 90 N·m which had a similar value obtained from an industrial hand-held pneumatic wrench. Transverse web stiffeners were used and located at the supports and mid-span.

2.2. Test setup, loading regime and instrumentation

The test setup is shown in Fig. 3. The load was applied by using a 250-t hydraulic actuator placed centrally above the secondary specimen. Steel roller supports of 80 mm in diameter were used and placed underneath the primary beams to assume simple and pinned supports. In the tests, clamps were used to fix the bottom flanges of the primary beam onto the roller bases. The rotation of primary beams during loading was deemed limited. Basic loading regime is given as follows:

a) loading up to 200 kN (50% of the design failure load in the first test) by 20 kN load increment,
b) unloading to 20 kN and re-loading to 200kN to observe the initial stiffness,
c) after yielding, 0.5 mm increment under displacement control and loading to failure.

Instrumentations of the tests are illustrated in Fig. 4. Strain gauges and LVDTs were used to monitor the strains of the BSCs and measure the deflections and rotations of the beams, respectively.

2.3. Experimental results

Mid-span deflection of the secondary beam, moment vs. rotation relationship, initial rotational stiffness and modes of failure of the specimen were obtained from the experiments. Behaviour of the specimen was further revealed by strain measurements. The deflection and rotation diagrams of the BSC connection system at concentrated loading are depicted in Fig. 5, where $\Delta_1\Delta_1$, $\Delta_2\Delta_2$, and $\Delta_3\Delta_3$ denote the mid-span deflection of the primary beam 1, primary beam 2 and secondary beam 3, respectively; θ_1 and θ_2 represent the rotations of the connections.

2.3.1. Mid-span deflection

The relationships between the total load and the mid-span vertical deflection of the secondary beam (Δ_3) obtained from two tests are depicted in Fig. 6. The deflection Δ_3 was the measurements of LVDT-4 without deducting the deflections (Δ_1 and Δ_2) of the primary beams. The curve for the 1st test shows fluctuations during the loading stage, mainly because slip of bolt occurred. This was expected because the first specimen was fabricated with propping. The fact that the curve for the 2nd test (without propping) shows no such fluctuation confirmed this. To study the effect of bolt slippage, the amount of bolt slippage was deducted from the first test, as indicated by the curve 'Test-1 Slip Removed'. The total shear resistance of the connections obtained was 450.1 kN and 455.7 kN from the first and second test, respectively, with

Fig. 2. Specimen assembly and components: (a) beam-beam connection, (b) secondary beam with welded end plates, (c) primary beams, BSCs and stiffeners before assembling.

Table 1
Components used for one beam-to-beam connection system.

Components	Profile (nominal)	Quantity	Material
Primary Beam	356 × 171 × 57 UB; length 1280 mm	2	S355
Secondary Beam	356 × 171 × 57 UB; length 1600 mm	1	S355
Block shear connector	152 × 152 × 23 UC; length 250 mm	2	S355
End plate	150 mm × 10 mm × 250 mm	2	S355
Bolt/nut	M20; fully-threaded; length 60 mm	24	Gr. 8.8
Stiffener for beam	80 mm × 10 mm × 330 mm	12	S355

a 1.2% difference, suggesting that nearly no resistance loss in the reassembled specimen with reused steel beams. The corresponding mid-span deflection was 7.8 mm (omitting bolt slip; approximating to span $L/250$) and 10.2 mm (approximating to span $L/190$), respectively. As it can be seen from the curves, the relationship between the total load and mid-span deflection was almost linear before a plateau was reached. The unpropped construction technique used for the second test eliminated large bolt slips and sudden load drop occurred in the early stage of the first test.

2.3.2. Moment vs. rotation

To assess the rotational stiffness of the connection, the bending moment and rotation were obtained from calculation. The applied moment at the connectors (150 mm away from the web of the primary beam) and the rotations of the connections were calculated by using the Eqs. (1)–(4) given as follows.

$$M = F/2 \times 0.15\ (\text{kN·m}) \tag{1}$$

$$\theta = (\theta_1 + \theta_2)/2\theta = (\theta_1 + \theta_2)/2\ (\text{mRad}) \tag{2}$$

$$\theta_1 = tan^{-1}[(\Delta_{LVDT2} - \Delta_1)/180] \times 10^3 \tag{3}$$

$$\theta_2 = tan^{-1}[(\Delta_{LVDT6} - \Delta_2)/180] \times 10^3 \tag{4}$$

The comparison of moment vs. rotation curves obtained from the tests are illustrated in Fig. 7. The average maximum moment was 34.0 kN·m (equivalent to a shear force of 226.7 kN), suggesting that the BSCs were sufficient to sustain the designed moment of 30 kN·m and shear force of 200 kN. Calculation data of the initial rotational stiffness is summarized in Table 2. Data points 1 and 2 denote the data corresponding to the points 1 and 2 in Fig. 7. The tested joint is classified as a nominally pinned joint by the initial rotational stiffness.

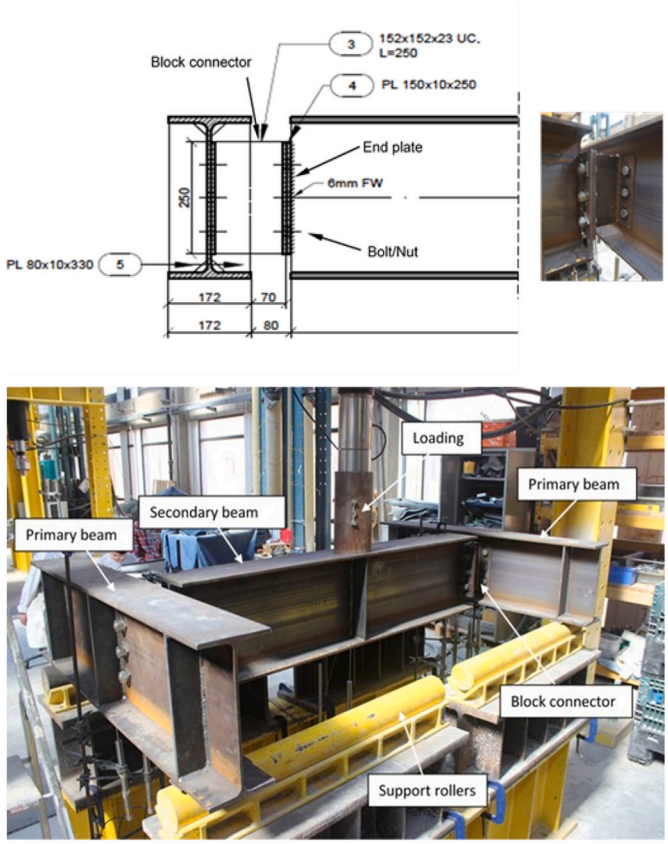

Fig. 3. Test setup.

2.3.3. Mode of failure

The governing mode of failure of the specimen was observed as web yielding followed by post-buckling of the BSC due to the forces transferred from the secondary beam through the end plates, as given in Fig. 8. The out-of-plane deformation of the connectors eventually caused rotation of the end plates and web yielding of the secondary beam at the weld toe. It should be noted that this torsional buckling of the secondary beam occurred after the peak load was attained, as shown in Fig. 6. There was no other obvious deformation observed in the bolts, the beams and the end plates after the test, as illustrated in Fig. 9. In the first test, due to propped construction technique was used, i.e. the specimen

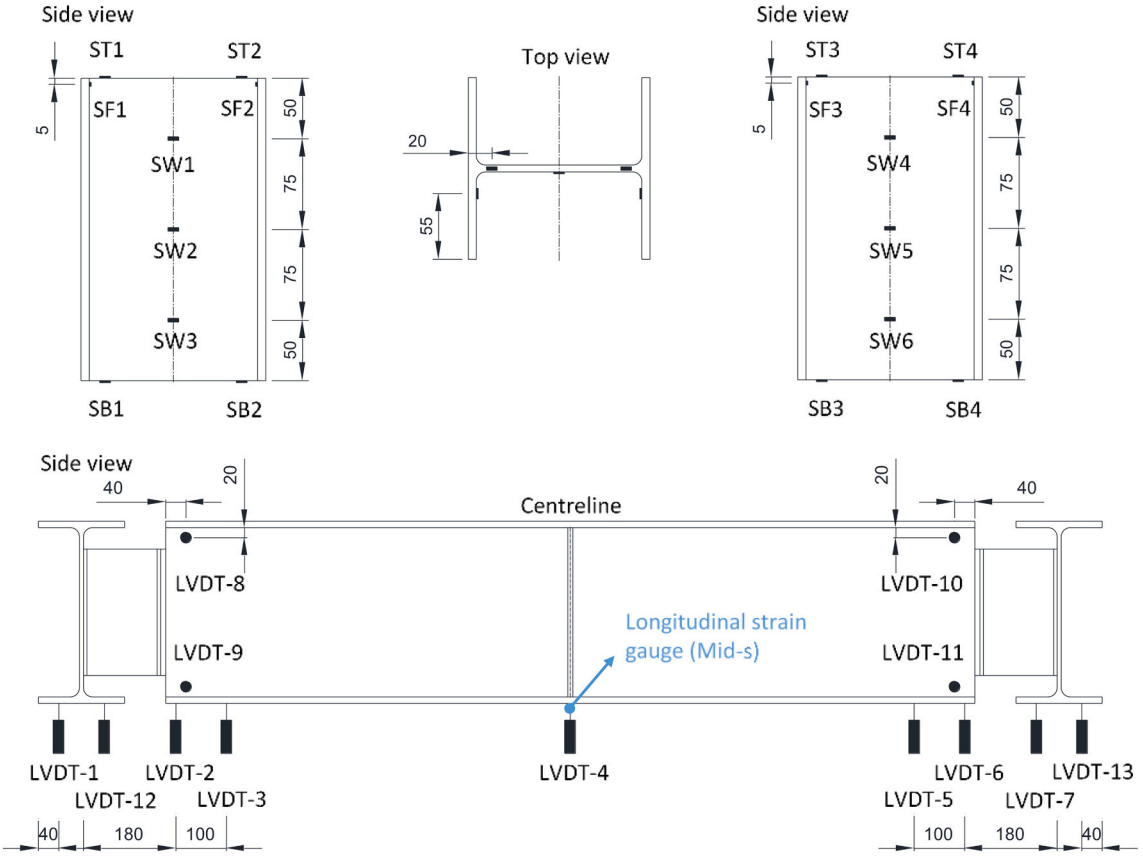

Fig. 4. Arrangement of strain gauges and LVDTs (dimension unit: mm).

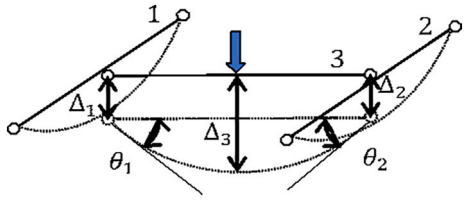

Fig. 5. Deflection and rotation diagrams.

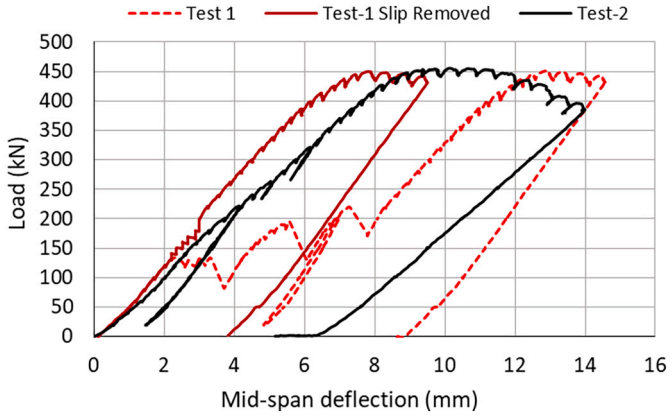

Fig. 6. Total load vs. mid-span deflection (secondary beam).

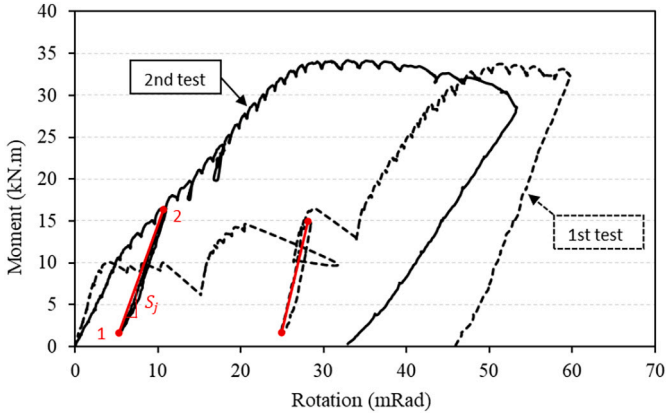

Fig. 7. Comparison of moment vs. rotation relationships.

Table 2
Calculation data of the initial stiffness of the specimens.

ID	Data point 1		Data point 2		Stiffness
	M (kN·m)	*R* (mRad)	*M* (kN·m)	*R* (mRad)	S_j (kN·m/mRad)
First test	1.63	5.28	16.36	10.65	2.74
Second test	1.67	24.91	14.96	28.09	4.18
Average					3.46

was assembled on the laboratory floor before it was lifted to the loading rig and clearances between the bolts and holes existed, and therefore bolts slippage occurred at the interfaces between the BSC to the end plates as well as to the webs of the primary beams, as shown in Fig. 9. In the second test, the specimen was assembled using unpropped

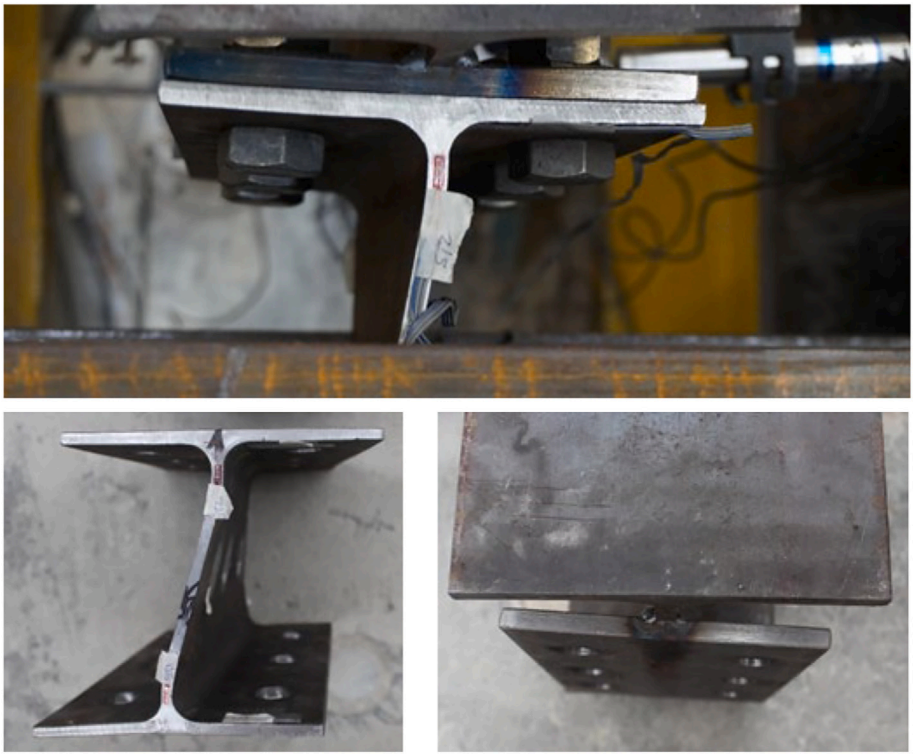

Fig. 8. Web buckling of the BSC and web yielding of the secondary beam/rotation of the end plate (compression).

Fig. 9. Dis-assembled steel components after tests and observed bolt slip during the first test.

construction technique, clearances were minimised and therefore no obvious slippage and sudden load drop were observed during the test. For both tests, the failure modes were as expected. It should also be noted that in reality it is likely that the top flanges of the beams would be attached to the floor slabs, which would serve as constraints to the beams. Therefore, it is likely that the post-peak torsional buckling may be eliminated with the presence of floor slabs.

2.3.4. Measured strains

The obtained maximum strain at the mid-span (strain gauge Mid-s) of the secondary beam was 1361 με, therefore it remained elastic, i.e. the secondary beam did not yield during the test and was in good condition for reuse. The strains in the BSCs suggested a non-symmetric behaviour of the specimen about the mid-span of the secondary beam especially after the connectors developed substantial deformation: the strains SF1 and SF2 were in compression whilst those at SF3 and SF4 were in tension; the connector at the left-hand side (SW1, SW2 and SW3) was basically under compression at high loads while the opposite side (SW4, SW5 and SW6) was under tension. The BSCs behaved as part of the beam element: the strains at ST2 and ST3 were initially in tension when the total load was below 180 kN, but were then beginning to yield in compression. The positions SB2 and SB3 exhibited significant low strains below the yield strain, which might be because the tensile force transferred from the secondary beam was sustained by the bolts. At lower loads, the strains at the first bolt line (SW1 and SW4) were in compression, while those at the middle and bottom bolt lines were extremely low. The strains (ST1 and ST4) were significantly below the yield strain at low loads and only started to yield in tension when the maximum load was achieved; the positions at SB1 and SB4 underwent compression in contrast. The connectors yielded at the later stage of the experiments, and then followed by buckling and twisting.

2.3.5. Remarks on demountability and reusability

After each test, the specimen was lifted by the crane and dis-assembled on the laboratory floor. The bolts were easily untightened by using a hand-held normal spanner. Beams and connectors were dismantled within a few minutes. Bolt slips can be well controlled by using unpropped construction technique. There was no obvious plastic deformation observed in the primary beams and bolts after the second

test. Thus, it is likely that they can be retrieved and re-used in their original forms for a third time. The main body of the secondary beam did not yield, however, minimum reprocessing such as cutting off the secondary beam ends may be needed for reuse because of the web yielding near the weld toe after ultimate loads. Noted that, when the loads are within serviceability limits which is one principle for design for reuse, no failure is expected from the secondary beam and other members, thus cutting off the ends are not necessary in this case. The BSCs are replaceable and can be sent to recycling after failure. Note that, if the main structure does not experience damage but will be dismantled for reuse in another building, the BSC system is adjustable to bridge different gaps between beams and the connecting members by changing geometries of the BSC, and all the beam components including end plates will be completely reusable.

3. Development of FE model and validation

3.1. Description of the modelling

Although full-scale specimen testing may provide reliable information for performance of connection systems, it is costly and time consuming. Therefore, following the bolted connection tests using Block Shear Connectors (BSC), nonlinear finite element software ABAQUS was used to develop the finite element model and simulate the structural behaviour of beam-to-beam connection systems. Considering the symmetrical configuration of the structure about the mid-span of the secondary beam, only a half of the specimen was modelled to improve computational efficiency. The main components of the FE model included the primary beam, the block connector, the secondary beam, the end plates, the beam web stiffeners and the bolts/nuts. All components were created separately and then assembled, as shown in Fig. *10*, to form the beam-to-beam BSC connection system. As listed in Table *1* and shown in Fig. *3* and Fig. *4*, the BSC was made from 152 × 152 × 23 UC steel section with length of 250 mm, the primary beam from 356 × 171 × 57 UB section with length 1280 mm and the secondary beam from 356 × 171 × 57 UB section with length 1600 mm. The BSC connected the web of the primary beam and the end plate (150 × 10 × 250 mm) of the secondary beam through M20 Gr. 8.8 bolts and nuts. The diameter of bolt holes was 22 mm. The dimensions of the stiffener plates were 80 × 10 × 330 mm.

3.2. Boundary conditions and element type/mesh

As shown in Fig. *11*, the boundary conditions of the FE model resembled those of tests. Load was applied at the mid-span of the secondary beam and four roller supports were placed underneath the ends of the primary beams. Three-dimensional eight-node solid brick elements with reduced integration (C3D8R) were adopted for all components. Once all the components of the connection system were assembled, appropriate contact interactions were defined between interacting surfaces of different components. Surface-to-surface contact was defined for contact pairs, which included bolt shank to bolt hole, BSC flange to primary beam web, BSC flange to end plate of the secondary beam, etc. The normal behaviour of contact was assumed to be 'hard contact' as this type of normal behaviour only allows little penetration of the nodes of the master surface into the salve surface. The penalty method was used to define the tangential friction with a coefficient of 0.2 between the steel components after a sensitivity analysis of the coefficients from 0.1 to 0.5.

3.3. Material properties

Elasto-plastic material properties were assumed for steel beams, end plates, stiffeners and BSCs. Their yield strength, Young's modulus and Poisson's ratio are 355 N/mm^2, 210 GPa and 0.3, respectively. For M20 Gr. 8.8 bolts and nuts, the yield strength and ultimate tensile strength were assumed to be 610 N/mm^2 and 850 N/mm^2, respectively. Young's modulus and Poisson's ratio adopted were 210 GPa and 0.3.

3.4. FE model validation and comparison

It was unrealistic to incorporate the complete true imperfection information of the specimen caused by manufacturing and assemblage, therefore, a vibration mode analysis was carried out for the connection system. The second mode mainly reflected the twisting of the connectors and the secondary beam with slight deformation on the web/flanges of both the primary and secondary beams. This vibration mode was introduced to simulate the imperfections of the connection system to improve the accuracy of the modelling. This imperfection was expected to cover the potential tolerances of the manufacture and assemblage of the specimen, e.g. non-straightness of the beams, twisting of the connectors and end plates, etc. The maximum imperfection introduced to the modelling included 0 mm (no imperfection), 1 mm, 2 mm and 3 mm. It was found that incorporation of the geometric imperfection mainly contributed to the decrease of the load at the post-peak branch. This indicates that the post-peak branch behaviour observed in the experiments might be initiated by geometric imperfections that were not fully covered by the FE models. Fig. *12* compares the predicted load vs mid-span displacement relationship with imperfection of 3 mm considered. Good agreement was obtained before the mid-span reached a displacement up to 12 mm. When the mid-span deflection reached 12 mm, the web of the block shear connectors deformed as buckling occurred in the web in the experiment. The predicted mode of failure also showed the twisting of the block web at this stage. Fig. *13* illustrates the predicted failure modes against the experimental observations. The deformation including twisting of the web of BSC and tilting of the end plate connected to the secondary beam were all well predicted, as those observed from experimental study. Fig. *14* compares the predicted and measured compressive strains at the top face of the web of the block shear connector. It shows that acceptable accuracy was obtained in terms of the slope of the initial increasing stage and the peak strain attained.

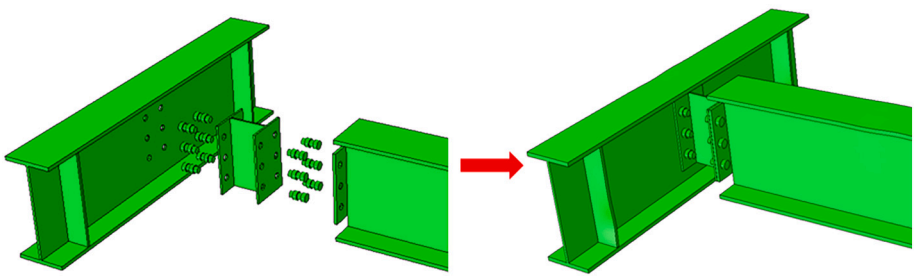

Fig. 10. FE Model of the components and connection system (half model).

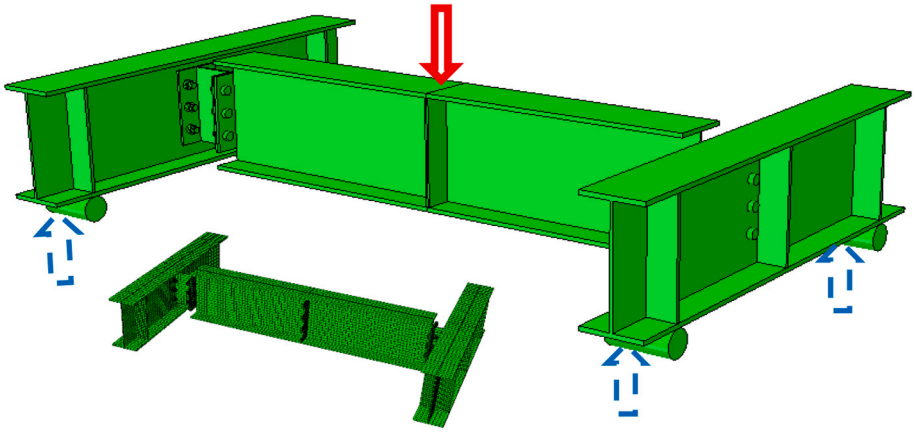

Fig. 11. FE model meshing and loading/support locations (full model).

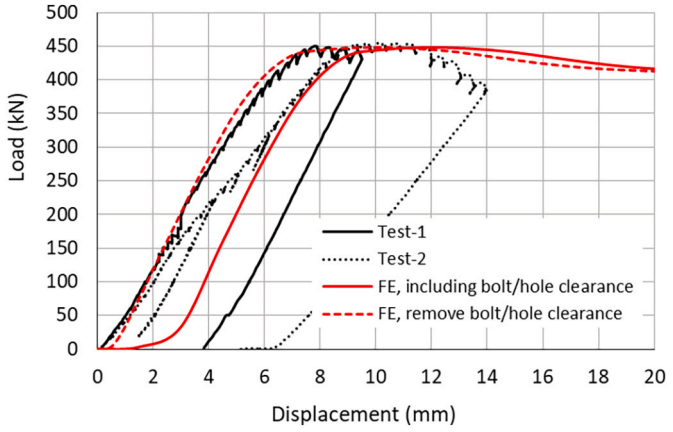

Fig. 12. Comparisons between FE predictions and experimental results (Load vs. displacement).

4. Parametric study

The parametric study aimed to further understand the structural behaviour and performance of this form of demountable beam-to-beam connection using BSC, when the material property, web thickness, flange thickness of BSC web and the initial stress of bolt after fixed are changed. The modelling validation in the previous section clearly shows the FE model developed successfully captured the main structural behaviour of the connection system, such as load versus mid-span deflection, moment versus joint rotation relationships, stress/strain development at the block shear connectors and deformations of connection components, this suggests that the developed model can be used for the parametric study.

4.1. Effect of steel strength of the BSC

Three steel grades, i.e., S275, S355 and S460, were adopted for the BSC whereas the steel grade of other members, including primary

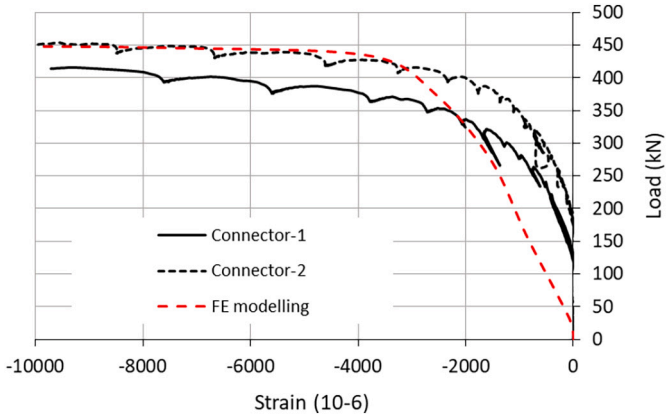

Fig. 14. Comparison between the predicted compressive strain at the web of the connectors and experimental result.

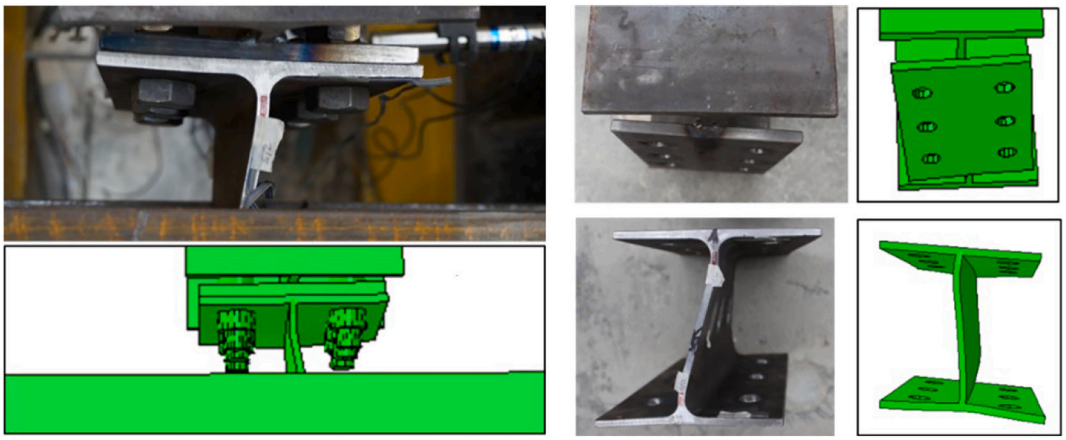

Fig. 13. Comparison between the predicted failures and experimental observations.

beams, secondary beam, end plate of secondary beam, were S355. The M20 G8.8 bolts/nuts were adopted.

Fig. 15 illustrates the comparison of the total load vs. mid-span deflection of the secondary beam. When increasing or decreasing the BSC steel grade to S460 or S275 from S355, the loading capacity of the connection system increased by 28.5% and decreased by 20.5%, respectively, compared to the capacity obtained from steel grade S355. In the design of beam coping, designers may have concerns about the end of the copped beams being prone to twisting and buckling as it is without a top flange or without both top or bottom flanges. The use of BSC with a higher steel grade than the secondary beam, however, might increase resistance of the connection and avoid such failure modes. This may be difficult to achieve if copped beams are used.

4.2. Effect of web thickness of the BSC

As seen from the tests, the failure mode of the connection system was characterized by the deformed web of the BSC, therefore the web of the BSC plays a crucial role in the connection system. The block shear connectors used in the tests were 152 × 152 × 23 UC sections. Its nominal web thickness is 5.8 mm, therefore three web thicknesses, i.e., 4.8 mm, 5.8 mm, 6.8 mm, were adopted in this parametric study. Fig. 16 compares the total load vs. mid-span deflection of the secondary beam. With the web thickness increasing, the loading capacity of the connection system increased significantly, whereas the stiffness at lower load stage was similar. The implication is that the use of BSCs with the secondary beams opens up the possibility for designers to change the web thickness of the BSCs or to weld additional stiffeners to the BSC web to prevent twisting and buckling that would otherwise occur at the end of coped beams.

4.3. Effect of flange thickness of the BSC

The nominal flange thickness of BSC used in the experimental study is 6.8 mm. Although by the experimental study, the main visible failure mode was observed at the web of the BSC, the flange also experienced deformation due to prying force applied to the flange through bolts. Therefore, the BSC flange might affect the load capacity of the connections. Therefore, three flange thicknesses, i.e., 5.8 mm, 6.8 mm, 7.8 mm, were considered, however, the comparison shown in Fig. 17 suggests that the thickness of the flange has minor effect on the connection loading capacity although BSC with flange of 5.6 mm shows slightly low maximum load.

4.4. Effect of initial stress of the bolts

M20 Gr. 8.8 bolts were selected as fasteners for the connection system. Bolt failure was not expected and observed in the experimental study. However, the tightness of the bolts/nuts might affect the overall behaviour and mode of failure of the connection system since all loads from the secondary beam will be transferred through the bolts/nuts to BSCs and then to primary beams. A torque of 90 N•m based on practice was applied to individual bolts in the experiments. Therefore, four different initial axial stresses 0 N/mm^2, 50 N/mm^2, 100 N/mm^2 and 150 N/mm^2, corresponding to the torques 0 N•m, 50 N•m, 100 N•m and 150 N•m, were selected to be applied to the shank of the bolts in this parametric study to observe the effect bolt stressing to the connection system.

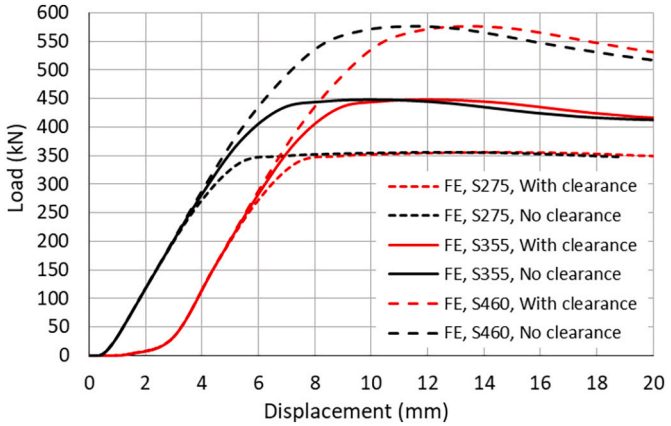

Fig. 15. Effect of steel strength of BSC on the loading capacity.

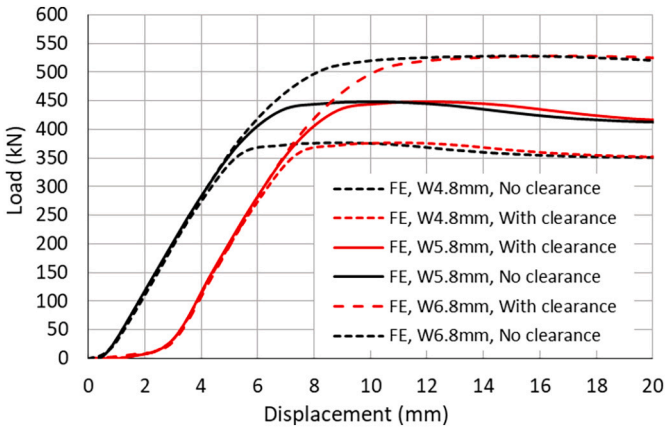

Fig. 16. Effect of BSC web thickness on the loading capacity.

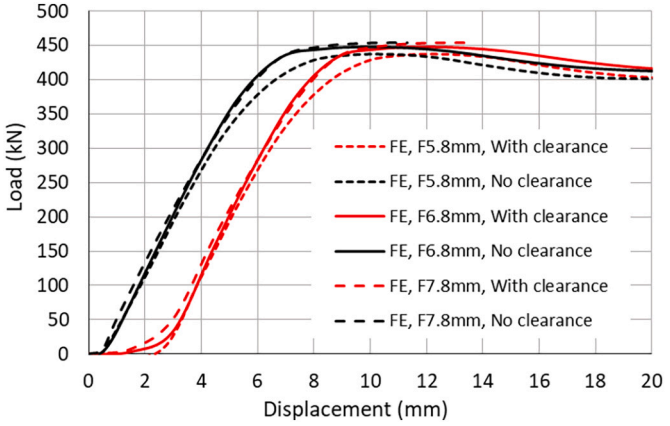

Fig. 17. Effect of BSC flange thickness on the loading capacity.

Fig. 18 shows the comparisons on the total load vs. mid-span deflection relationship of the secondary beam. Obviously with the increasing of the initial tensile stress, the loading capacity of the connection system increased significantly. With the increasing of the tightness, the initial slip between the interfaces of the endplate, the connector and the web of the primary beam at low loads was reduced. The comparison indicates that when the initial tensile stress was below 50 N/mm^2, it had little effect on the load capacity and failure mode.

5. Conclusions

Experimental and numerical studies on an innovative 'Block Shear Connector' connection system were presented in this paper. Shear resistance, moment-rotation and failure behaviour of the connections were obtained. Ease of demountability and the reusability of the steel components were highlighted. A further parametric study was conducted on key parameters that affect the behaviour of the connections. The following conclusions may be made.

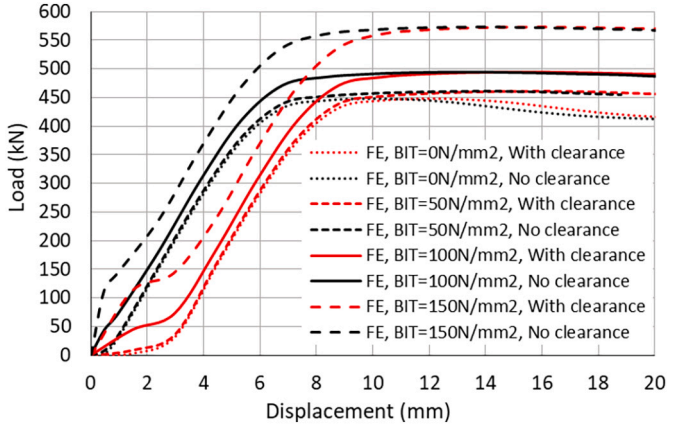

Fig. 18. Effect of initial axial stress of bolt shank on the loading capacity.

a) The Block Shear Connectors (BSC) performed as part of the secondary beam: under compression at the top and under tension at the bottom.
b) The mode of failure was web yielding followed by post-buckling of the BSC caused by compression.
c) Bolt slip occurred after the friction was overcome during the first test and the maximum slip was determined by the sum of the bolt hole clearances; slippage can be minimised by using unpropped construction technique.
d) The selected 152 × 152 × 23 UC connectors were sufficient to meet the designed moment and shear force under Ultimate Limit State.
e) The proposed connection system was easy to dismantle, the BSC was replaceable and most of the components can be reused on their original forms whilst the secondary beam may need minimum reprocessing for reuse such as cutting off the beam ends near the weld toe in practice. In the scenarios when the structures do not experience damage but are deconstructed, for example, loads are within serviceability limits, all the structural components can be reused in another building by adjusting the BSCs selected if necessary.
f) The finite element models developed may be used to predict and capture the main structural behaviour and failure modes of the block connection system.
g) The steel strength, web thickness of the BSC significantly affected the load capacity of the designed block connection system. However, the flange thickness of the BSC had a minor effect within the limited scope of this study. The implication is that using BSCs of a higher steel grade or increasing the web thickness of the BSCs may increase the resistance of the connection and prevent failure modes, such as twisting and buckling that would other occur at the end of coped beams. Additional stiffeners may also be welded to the BSCs if the web thickness is limited by the dimensions of the BSCs.
h) The tightness of the bolts/nuts affected the load capacity and behaviour of the block connection system significantly on the load capacity and bolt slippage. When the initial stress was below 50 N/mm^2, it had a minor effect but larger initial slippage. According to the parameter study, it is suggested that higher torque, such as 90 N·m for the current practice, is adopted when tightening the BSC bolts/nuts to increase the resistance of the BSCs and to reduce the initial slippage.

Authorship statement

This paper was prepared by the above five authors. They share all data and achievements.

Declaration of Competing Interest

This paper has no conflict of interest with other people, organizations.

Data availability

Data will be made available on request.

Acknowledgement

The research leading to these results is part of a joint project of the University of Bradford, the University of Luxemburg, the Technology University of Delft, the Steel Construction Institute, Tata Steel, Lindab S. A., BmS and AEC3 Ltd. The authors gratefully acknowledge the funding received from the European Commission: Research Fund for Coal and Steel (RFCS-2015, RPJ, 710040). In addition, deep appreciation to Mr. Stephen Robinson for his work done in the laboratory.

References

[1] M. Sansom, N. Avery, Briefing: reuse and recycling rates of UK steel demolition arisings, Proc. Instit Civ. Eng. Eng. Sustain. 167 (2014) 89–94.
[2] T. Norgate, S. Jahanshahi, W. Rankin, Assessing the environmental impact of metal production processes, J. Clean. Prod. 15 (2007) 838–848.
[3] D.A. Nethercot, Towards a standardisation of the design and detailing of connections, J. Constr. Steel Res. 46 (1998) 3–4.
[4] M. Kidd, R. Judge, S.W. Jones, Current UK trends in the use of simple and/or semi-rigid steel connections, Case Stud. Struct. Eng. 6 (2016) 63–75.
[5] BCSA, Tata Steel and SCI, Publication No. P358 Joints in Steel Construction: Simple Joints to Eurocode 3, The Steel Construction Institute & The British Constructional Steelwork Association Limited, Ascot, UK, 2014.
[6] M.D. Engelhardt, Reinforcing of steel moment connections with cover plates benefits and limitations, Eng. Struct. 20 (1998) 510–520.
[7] H. Gervasio, L. Simoes da Silva, L. Borges, Reliability assessment of the post-limit stiffness and ductility of steel joints, J. Constr. Steel Res. 60 (2004) 635–648.
[8] L.R.O. Lima, L.S. Silva, P.C.G. Vellasco, S.A.L. Andrade, Experimental evaluation ofextended endplate beam-to-column joints subjected to bending and axial force, Eng. Struct. 26 (2004) 1333–1347.
[9] J.M. Cabrero, E. Bayo, Development of practical design methods for steel structures with semi-rigid connections, Eng. Struct. 27 (2005) 1125–1137.
[10] A.B. Francavilla, M. Latour, V. Piluso, G. Rizzano, Design of full-strength full-ductility extended end-plate beam-to-column joints, J. Constr. Steel Res. 148 (2018) 77–96.
[11] G. Shi, Y.J. Shi, Y.Q. Wang, Behaviour of end-plate moment connections under earthquake loading, Eng. Struct. 29 (2007) 703–716.
[12] J. Lee, H.M. Goldsworthy, E.F. Gad, Blind bolted moment connection to unfilled hollow section columns using extended T-stub with back face support, Eng. Struct. 33 (2011) 1710–1722.
[13] M. Gerami, H. Saberi, V. Saberi, A.S. Daryan, Cyclic behavior of bolted connections with different arrangement of bolts, J. Constr. Steel Res. 67 (2011) 690–705.
[14] C. Díaz, P. Martí, M. Victoria, O.M. Querinb, Review on the modelling of joint behaviour in steel frames, J. Constr. Steel Res. 67 (2011) 741–758.
[15] C. Zhu, K.J.R. Rasmussen, S. Yan, Generalised component model for structural steel joints, J. Constr. Steel Res. 153 (2019) 330–342.
[16] L.G. Jia, Q.R. Li, R. Bi, Y. Dong, Behaviour of castellated beam-to-column end-plate connection under monotonic load, Structures 34 (2021) 4616–4633.
[17] S. Yan, K.J.R. Rasmussen, Generalised component method-based finite element analysis of steel frames, J. Constr. Steel Res. 187 (2021), 106949.